The Infrared Luminosity Function of Galaxies

Caroline Huang

Received _____; accepted _____

ABSTRACT

We used spectroscopic data from the Sloan Digital Sky Survey (SDSS) and photometric data from the Wide-Field Infrared Survey Explorer (WISE) to create a luminosity function of almost 200,000 galaxies in the WISE1 (W1) 3.4-micron band. This was made possible by the high-signal-to-noise ratios of WISE data, which allowed us to create a luminosity function which depended on only the selection function in SDSS. We compared these results with the $r^{0.1}$-band luminosity function to find that there is a significantly higher luminosity density in the W1-band, with $j \approx 6.605 \times 10^8 h\, L_\odot\, \mathrm{Mpc}^{-3}$ in the infrared W1-band and $j \approx 1.75 \times 10^8 h\, L_\odot\ \mathrm{Mpc}^{-3}$ in the optical $r^{0.1}$-band. Young, massive stars emit most of their light in optical wavelengths, but contain only a small amount of a galaxy's stellar mass, contributing a disproportionate amount of light to stellar mass. As a result, the W1-band allows us to get a better estimate of the overall stellar mass, since the galaxy luminosity function in the infrared and near-infrared is less sensitive to recent star formation histories and extinction due to interstellar dust. The color-magnitude diagrams from both bandpasses indicate that the most luminous galaxies are also redder in color.

1. INTRODUCTION

The galaxy luminosity function (LF) describes the distribution of luminosities for a galaxy population and allows us to study the evolution of galaxies over time. Infrared (IR) and near-infrared (NIR) luminosity functions are especially useful because they allow us to get more reliable estimates of stellar mass (Bell and de Jong 2001). At optical wavelengths, the flux from a galaxy is dominated by the emission from the most massive stars, which make up only a small fraction of the galaxy's stellar mass while providing most of its optical luminosity. Thus galaxies with higher star formation rates will emit more of their light in bluer wavelengths since they contain a larger population of young, massive stars. Besides the dependence on star formation histories, optical observations are also hampered by their sensitivity to extinction due to interstellar dust in both our galaxy and in other galaxies (Kochanek et al. 2001).

Both of these effects are diminished at infrared wavelengths, so studying the luminosity function in the infrared causes our data to be less affected by recent star formation. At longer wavelengths, there is less extinction and even dusty galaxies are almost transparent in the K-band (Kochanek et al. 2001). The mass-to-light (M/L) ratios also vary less over a range of star formation histories so that while the bluer end of the optical regime has up to a range of a factor of 10 in M/L, in the NIR, M/L ratios only vary up to about a factor of 2. As a result, a galaxy's NIR luminosity provides a more representative picture of its stellar mass (Bell et al. 2003).

While previous work with data from the SDSS has produced optical luminosity

functions containing data on hundreds of thousands of galaxies Blanton et al. (2003), infrared galaxy surveys have been limited by the difficulty of acquiring large samples. The WISE telescope's comprehensive coverage of the sky in the infrared bands allows us to create a luminosity function in the infrared that incorporates data on many more galaxies than was previously possible. Earlier infrared luminosity functions, which relied on data gathered from ground-based sky surveys such as 2MASS contained significantly fewer galaxies, with ∼4912 galaxies in Kochanek et al. (2001) and ∼6282 galaxies in Bell et al. (2003).

Both of these earlier galaxy surveys found that studying the luminosities in the K-band, a bandpass centered on 2.2 μm, allows for cleaner estimates of the galaxy's stellar mass. The K-band is approximately 5-10 times less sensitive to extinction and light from young stellar populations, allowing it to give us a better measure of stellar mass in galaxies close to us (Bell & de Jong 2001).

The first WISE data release overlaps with the SDSS large scale structure samples for nearly 200,000 galaxies. The WISE W1-band (3.4 μm) corresponds roughly to the K-band in ground-based surveys. Since it is a space telescope, it does not have to contend with the noise that ground-based detectors pick up from infrared energy from sky brightness. The last infrared survey in space before WISE, the Infrared Astronomical Satellite (IRAS) was launched in 1983. It was also able to survey the entire sky, but WISE has sensitivities that are about a factor of 1,000 times higher than IRAS. This provides us with the unique opportunity to further study the infrared luminosity function with a much more comprehensive and sensitive data set.

2. SDSS DATA

2.1. Overview

The SDSS (York et al. 2000) is an imaging and spectroscopic redshift survey using a dedicated 2.5 m telescope located at Apache Point Observatory, Sunspot, New Mexico (Siegmund et al. 2003). The telescope uses a drift-scanning, mosaic CCD camera (Gunn et al. 1998) to image the sky in five bands (u, g, r, i, z; Fukugita et al. 1996) between 3000 and 10000Å. The spectroscopic measurements are made using a spectrograph with 640 fibers that is attached to the same telescope as the imaging camera. After beginning its data collection in 2000, it has mapped more than 35% of the sky, and the most recent data release, Data Release 8, covers about 14,555 square degrees.

We use data from the Large Scale Structure (LSS) samples in the NYU Value-Added Galaxy Catalog (NYU-VAGC) to construct the $r^{0.1}$-band LF (Blanton et al. 2005). The sample used from the LSS–the bsafe25 sample–consists of data taken from the Sloan Digital Sky Survey's (SDSS) seventh data release. The sample contains 516,685 galaxies with a constant flux range of $14.5 \leq r^{0.1} \leq 17.6$ mag that cover approximately 6955 square degrees of the sky. Fainter galaxies do not have uniform spectroscopic coverage in SDSS while brighter galaxies can suffer from deblending issues. Deblending issues may occur when the pipeline mistakes one bright galaxy for multiple objects and essentially splits it (the "parent" object) into separate objects (the "children"). The sample we chose does not contain collision corrections, which are explained in greater detail in Section 2.2. Since there are no collision corrections, we can take a subset of the data from the sample. If we had

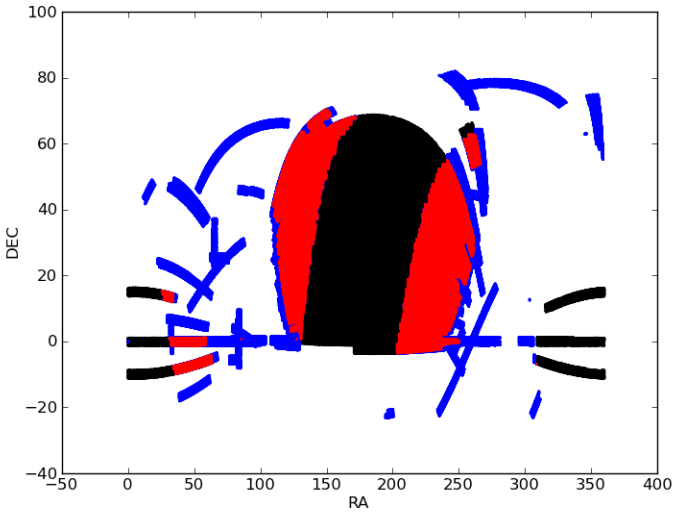

Fig. 1.— Every point on this plot is a galaxy from the SDSS. However, the black areas indicate the galaxies that were only covered by the SDSS and not the Large Scale Structure (LSS) sample used in this paper. The blue areas are the locations of the galaxies from WISE that had no match with galaxies from the LSS. The red portions indicate the overlap of galaxies from LSS and WISE–these are the galaxies for which we have both redshift measurements (from SDSS) and infrared photometry data (from WISE). This is a total of 199,465 galaxies.

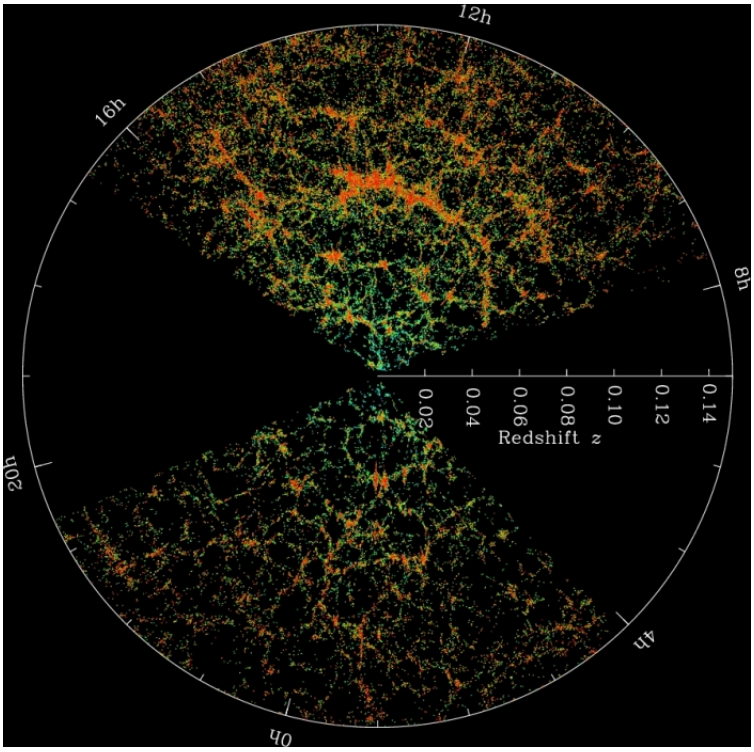

Fig. 2.— A pie diagram showing the redshift and right ascension of data from SDSS plotted for a narrow band of declination values. The large-scale structure of the universe is visible here. From: http://www.sdss.org.

collision corrections included in the sample, then we would not be able to take a smaller portion of the sample to use to study with WISE data, since the collision corrections would no longer be accurate for a subset of the galaxies.

Redshift limits were placed on the $r^{0.1}$-band galaxies that limited them to $5000 < cz < 75,000$ km s^{-1}. The high redshift limit was set to limit the noise in determining the normalization. The low redshift limit was set in order to avoid accidentally deblending large nearby galaxies (Blanton et al 2005).

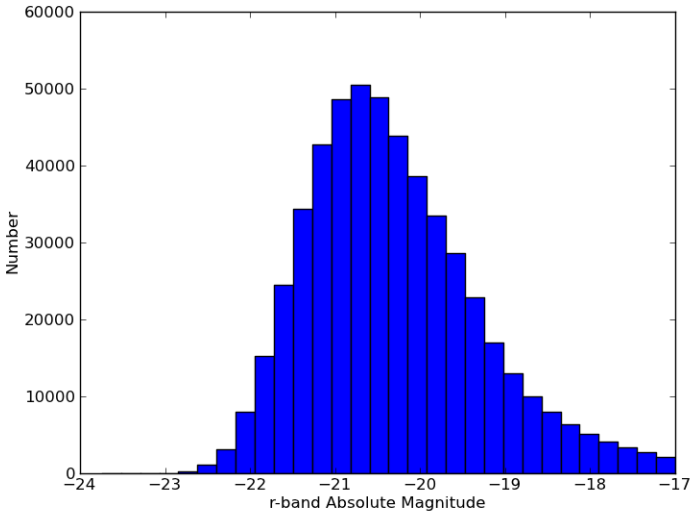

Fig. 3.— The distribution of galaxies in the full LSS sample by luminosity, without weights. There are fewer galaxies of low luminosity in our survey. However, because these can only been seen in a small volume of space close to us, they actually have greater number density than more luminous galaxies.

The data in the SDSS sample had a bandshift of $z = 0.1$ (defined using the same variable as redshift, but distinct from redshift), while the WISE data did not have a bandshift. The bandshift tells us what we chose to use as the rest-frame bandpass. If we had a bandshift of 0, then we are looking at some object as we would observe it in our rest-frame bandpass. Picking a bandshift of $z = 0.1$ means that we are looking at light that has 10% shorter wavelength than the rest-frame bandpass would have without a bandshift, so the $r^{0.1}$-band is 10% shorter in wavelength than the r-band. This would give us the same result as if we had blueshifted the filter out to $z = 0.1$. This means that we are observing the galaxies relative to how they

would appear if we were at redshift $z = 0.1$ (Blanton et al. 2003).

2.2. Sampling Rate

Besides the flux limits, there are also galaxies missing from the spectroscopic data due to a lack of fibers in dense regions on the sky, spectroscopic failures, and fiber collisions. We can account for these types of effects by making sector weights and fiber collision weights (Blanton et al. 2001).

Fiber collision weights are made to account for the missing galaxies that did not receive redshift measurements because they were too close to another galaxy. While the optical fibers used in recording the spectroscopic data were relatively narrow (about 3″) the holes themselves are much larger, because of the ferrules–the plugs–that hold the optical fibers in place. They span a diameter of about 55″. Thus, if two galaxies are within 55″ of each other, their fibers would collide and only the redshift of one could be recorded. In order to account for this, we assign to each galaxy a collision weight equal to the number of galaxies within the 55″ collision radius–a collision group–since only one galaxy in each collision group will receive a redshift measurement. If one galaxy caused another not to be recorded, we assign it a double weight. In some cases, we are able to observe more than one galaxy in a particular collision group, perhaps because some regions of the sky were observed multiple times. In that case, if we have 3 galaxies whose fibers all collide, and 2 eventually get observed, our collision weight for these two galaxies would be 1.5 each.

It should be noted that these collision weights will only make a difference if the typical luminosities of the galaxies that caused fiber collisions were different from the typical luminosities of the other galaxies (Blanton et al. 2001). The collision weights of the bsafe galaxies were extracted after calculating the collision weights for all of the SDSS galaxies with recorded redshifts. These weights were also applied to make the LF for the intersection of WISE and LSS data.

The sector weights allow us to calculate a "sampling rate" (Blanton et al. 2001). That is, the probability that any given object in each "sector" would receive a redshift measurement. The sectors are pieces of spherical polygons that are defined by a region which is a unique set of overlapping plates. These sector weights were made by first calculating the sampling rate in each region covered by a unique combination of plates. For example, for two slightly overlapping and adjacent plates (in a manner similar to a Venn diagram), the regions covered by each plate and the intersection between both plates would each be a different sector, making a total of three sectors. Each of these sectors was then assigned a sampling rate that is the fraction of galaxies in each sector that had received a redshift measurement over the number of galaxies that had been assigned to a sector. In practice, we would weight by the inverse of our sector weight. The sample we used, however, has the sector weights incorporated into the $V_{\rm max}$ values–the maximum volume of space over which our galaxies can be seen. Since we will later need to weight our luminosity function by $1/V_{\rm max}$ we do not also weight them by the sector weights.

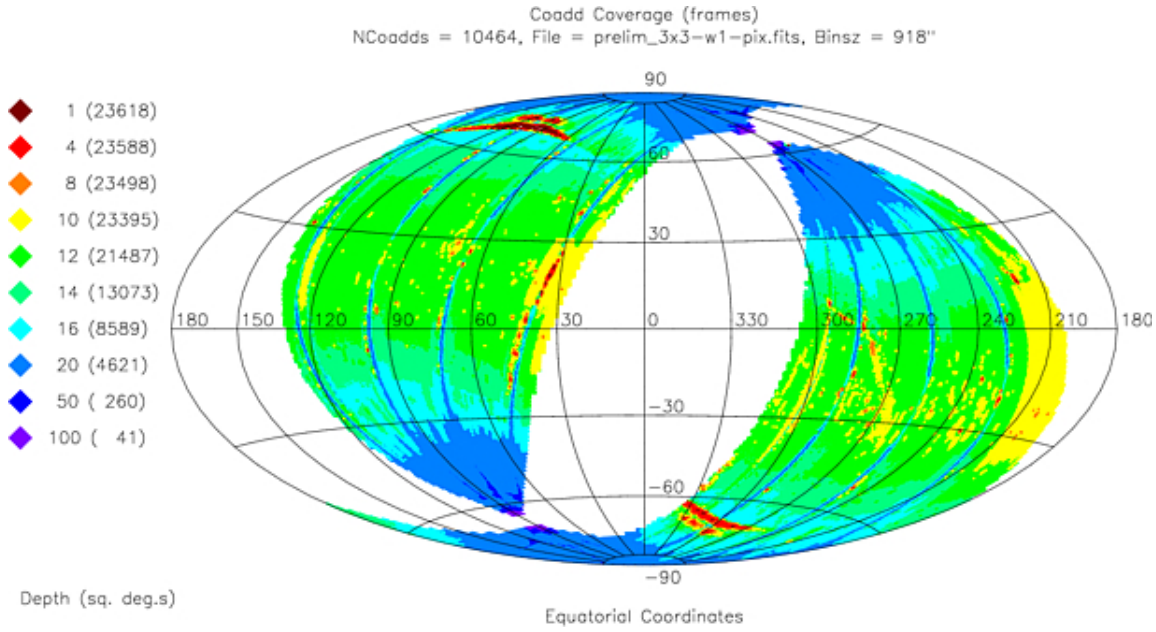

Fig. 4.— An equatorial Aitoff projection map of the sky that shows the area covered by WISE in the first data release, with the colors denoting the average number of times an area, binned by $15' \times 15'$ was covered by the 7.7/8.8 second exposures. From: http://wise2.ipac.caltech.edu/docs/release/prelim/index.html#skycover

3. WISE DATA

3.1. Overview

WISE is a NASA mission that seeks to continue the work done by previous infrared sky surveys like the Two Micron All Sky Survey (2MASS) by mapping the whole sky. WISE was able to complete its first mapping of the full sky on July 17, 2010, and was able to make another full mapping of the sky before it exhausted its cryogen supply (Wright et al. 2010). Mainly because WISE is a space telescope,

and not a ground-based survey, it has been able to survey the entire sky with much greater sensitivity than any previous infrared sky survey. WISE mapped the sky in the 3.4 (W1), 4.6 (W2), 12 (W3), and 22 (W4) μm wavelength bands with an angular resolution of 6.1″, 6.4″, 6.5″, and 12.0″ in the four bands respectively. This gives WISE resolution 5 times better than Infrared Astronomical Satellite (IRAS) at 12 and 25μm and hundreds of times better than the Cosmic Background Explorer (COBE) at 3.5 and 4.9μm.

WISE's sensitivities vary based on position in the sky because of differences in the telescope's depth-of-coverage (explained in greater detail below) and zodiacal foreground emission (zodiacal light is the diffuse white light that extends from around the Sun along the ecliptic), with both improving near the poles. WISE's four detector arrays have 5-sigma source sensitivities up to 0.08, 0.11, 1 and 6 mJy in each of the four filters. Compared to previous all-sky surveys in the same wavelengths, COBE had point-source sensitivities of about 60 Jy at 3.5μm and 50 Jy in 4.9μm, IRAS had sensitivities of 0.2 Jy at 12 and 25μm, and AKARI had sensitivities of 50 mJy at 9μm and 90 mJy at 18μm. It is approximately 1,000 times more sensitive than IRAS and almost 500,000 times more sensitive than COBE.

Unlike WISE, which surveys the entire sky, the Spitzer Space Telescope (SST), an infrared space observatory that was launched in 2003 looks more deeply into targeted patches of the sky. Spitzer performed imaging and spectroscopy in $3 - 180\mu$m and had a band at 3.6μm. Spitzer allows us to study galaxies at a higher redshift in the infrared than WISE, while WISE is a shallower but broader survey that allows us to study galaxies at low redshift.

The preliminary data from WISE was released on April 14, 2011 and covers approximately 23,600 deg^2 or 57% of the sky. It included data from the first 105 days of WISE survey observations, which spanned from January 14, 2010 to April 29, 2010. The data used in this paper were from the WISE1 (3.4-micron) band. The SDSS data from our large scale structure sample were matched to the first data release from the WISE telescope, resulting in a total of 199,466 galaxies that appeared in both samples (with matching done by Blanton, private communication). Using the data from the W1-band we constructed an infrared LF. This roughly corresponds with the K-band used in ground-based surveys, which is centered on 2.2μm.

Figure 4 shows the scanning strategy adopted by WISE, which orbited the Earth such that it was constantly able to observe on the side opposite from the Sun. Thus, the frame depth-of-coverage (average number of frames contributing to each point on the sky) increases towards the ecliptic poles. We can see from Figure 4 that on average, 12 independent exposures contribute to each point on the sky close to the ecliptic plane with a maximum of approximately 260 frames at the poles.

Each exposure for W1 and W2 lasted approximately 7.7 seconds, and 8.8 seconds for W3 and W4. All four of the WISE bands were imaged simultaneously. The areas of unusually low average frame depth-of-coverage were the result of exposures being filtered out due to lower quality because of contamination from scattered moonlight, degradation of the image quality as a result of the flight system motion, and other events.

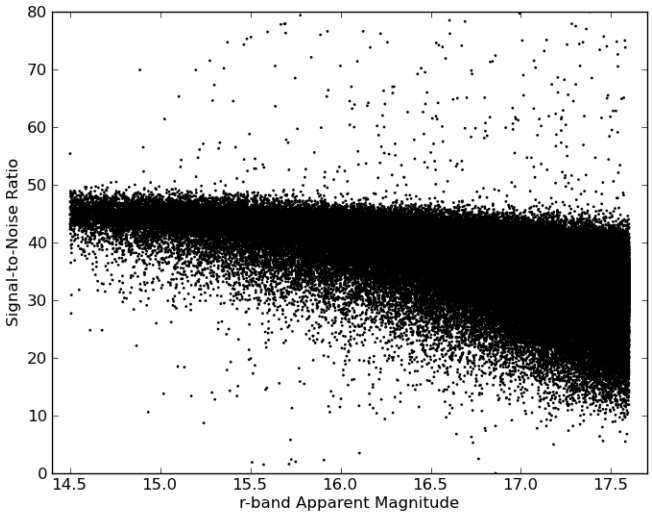

Fig. 5.— The point-source signal-to-noise ratio of the WISE data plotted against the $r^{0.1}$-band apparent magnitudes from SDSS. This shows a high signal-to-noise ratio for all of the galaxies in our sample. The actual signal-to-noise ratio, since our galaxies are not point sources, is likely to be even higher.

3.2. WISE Signal-to-Noise Ratios

We plot the point-source signal-to-noise ratios of the WISE data of all the galaxies that were in the LSS sample in Figure 5. This was the value of the ratio of flux to flux uncertainty for the WISE1 profile-fit photometry measurement. This shows that there are high signal-to-noise ratios (above 10) for all of the galaxies in SDSS that had been covered by our WISE data. As a result, we did not have to remove any galaxies from our calculations. All of the objects in the bsafe sample that overlapped with WISE have reliable photometry, so their selection function is determined only by the constraints of SDSS.

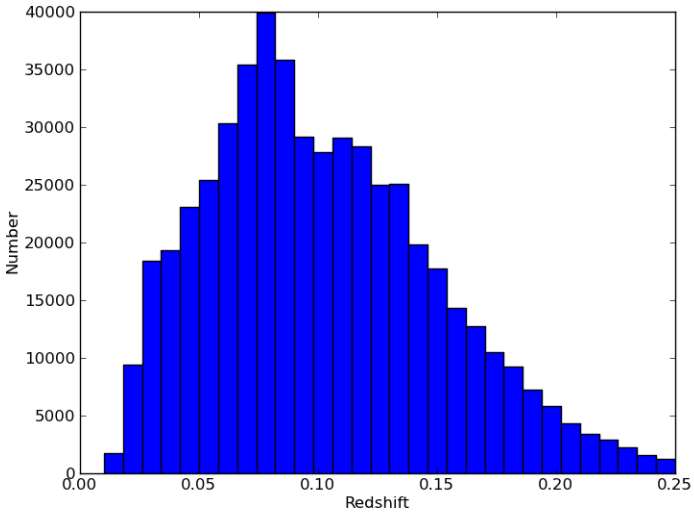

Fig. 6.— The number of galaxies in each redshift range of our full large scale structure sample, which shows that the most important redshift range is around $0.05 < z < 0.10$.

Because we used the signal-to-noise ratio for point sources, at lower apparent magnitudes the real signal-to-noise is likely to be higher than is shown in Figure 5. Since these WISE magnitudes were calculated using a fixed aperture radius, at lower apparent magnitudes more of the galaxy's flux will be outside of the aperture radius. The radius of the aperture was likely not large enough to contain all of the flux from a brighter galaxy.

4. METHODS

4.1. Distance Modulus and K-Correction

To convert the data from the apparent magnitude, m, to the absolute magnitude, M, we needed to calculate the luminosity distance and K-correction. The relation between m and M is

$$M = m - \mathrm{DM}(z) - K(z) \tag{1}$$

where $\mathrm{DM}(z)$ is the distance modulus and $K(z)$ is the K-correction, and z is the redshift (Blanton et al. 2001). The distance moduli were created by using the luminosity distance, D_L, where

$$\mathrm{D_L} = (1 + z_i) \int_0^{z_i} \frac{c}{H_0 \sqrt{\Omega_\mathrm{m}(1+z)^3 + \Omega_\Lambda}} dz \tag{2}$$

and c = speed of light, z_i is the redshift of an object with luminosity distance $\mathrm{D_L}$, $H_0 = 100h$ (km/s/Mpc), $\Omega_m = 0.3$, and $\Omega_\Lambda = 0.7$. We also choose to use $h = 1$. Then the distance modulus, $\mathrm{DM}(z)$ becomes

$$\mathrm{DM}(z) = 5 \log \frac{\mathrm{D_L}}{10 \text{ pc}} \tag{3}$$

The distance moduli were calculated using numerical integration. The redshifts for our galaxies were taken from the SDSS spectroscopic data.

The K-corrections correct for the fact that sources which are observed at different redshifts are compared with other objects that are at different rest-frame wavelengths. The K-corrections help relate a source's rest-frame absolute magnitude

in one bandpass with the observed apparent magnitude of the same source in another bandpass (Hogg et al. 2002). K-corrections were included in the SDSS absolute magnitudes, but we did need to make approximate K-corrections for the WISE data.

If we consider a source that was observed at redshift z, this means that we observed a photon with frequency ν_0 that was emitted at a source frequency ν_e with the following relationship

$$\nu_e = (1+z)\nu_0 \ . \tag{4}$$

To calculate the K-corrections properly we would have to have an accurate description of the source flux density, the standard-source flux densities, and the bandpass functions. However, for this paper, we assume that the spectral energy distribution (SED) in the infrared wavelength range does not vary significantly. An object's spectral energy distribution is the function of an object's brightness in different wavelengths. In spite of the fact that we are still comparing objects at different redshifts from each other in the same observed-frame bandpass (meaning that we are looking at different rest-frame bandpasses), we make an approximate K-correction that assumes that the spectral energy distribution is the same for all galaxies. This SED then has a constant flux per unit frequency over our frequency range. Usually our K-corrections would depend on the SED of each source, but since we have assumed that all the sources have the same SED, and that the SED has constant flux density over our frequency range, we can take

$$K(z) = -2.5 \log \left[\frac{(1+z)\mathrm{L}_{\nu_e}(z)}{\mathrm{L}_{\nu_0}} \right] \ . \tag{5}$$

Where $L_{\nu_e}(z)$ is the luminosity of the source at redshift z in the emitted frequency, ν_e, and $L_{\nu_0}(z)$ is the luminosity of the source in the frequency, ν_0 that we detect it. Since we have assumed a constant flux density over our frequency range, $L_{\nu_e}(z)$ will be equal to L_{ν_0}. Then our equation simplifies to

$$K(z) = -2.5 \log(1 + z). \tag{6}$$

This was the approximate K-correction that we used for our WISE data.

4.2. Calculating the Luminosity Function

The galaxy luminosity function tells us the number density of galaxies of a certain magnitude in a certain volume of space. We make a histogram of the number density of galaxies in a certain luminosity range in a certain amount of space, and the luminosity function parameters are calculated by fitting a Schechter function to the shape of the histogram. Because the most luminous galaxies can be detected to larger distances, when we survey the sky in a range of apparent magnitudes, our surveys are overall biased against less luminous galaxies. Galaxies whose apparent magnitudes are too low fall into our flux limits are left out of the sample so the less luminous galaxies can only be seen if they are fairly close to us, while the more luminous galaxies can be seen from much farther away. This means that when we are looking at more luminous galaxies we are surveying a larger volume of space than when we look at less luminous galaxies. To account for these effects, we weight each galaxy by $1/V_{\max}$ where $V_{\max}$ is the maximum volume of space over which the galaxy could be seen given the apparent magnitude limits of our survey. More

luminous galaxies will have larger $V_{\max}$ values. Since less luminous galaxies have more weight, this also means that we actually have a comparatively small number of less luminous galaxies in our sample. This can be seen by comparing the r-band LF (Figure 13) to the histogram of the galaxies in each absolute magnitude range without weights (Figure 3).

In addition to weighting each galaxy by $1/V_{\max}$, we also weight each galaxy by its collision weight, w_c, over the average collision weight. Even though sector weights are necessary to accurately calculate the luminosity function, we do not weight the luminosity function by the sector weight since they have already been incorporated in the $V_{\max}$ values.

For the WISE luminosity function, we use apparent magnitudes that were found using WISE's "standard" aperture magnitude. These magnitudes were found using circular apertures $8.25''$ in radius that were centered on the position of the source. This radius is probably too small for the brighter galaxies from our SDSS sample, but large enough for the dimmer galaxies. Using the apparent magnitudes from the WISE data, we converted them into absolute magnitudes with the formula given in Section 4.1. These luminosities are then weighted, as the optical galaxy luminosity functions were, by $1/V_{\max}$. However, the $V_{\max}$ values had been calculated for a much a larger volume of space than the intersection of the WISE and SDSS data. To correct for this, we weight the $V_{\max}$ values by the inverse of the fraction of the sky covered by the intersection of the WISE and SDSS data. For this we use the number of galaxies in the original SDSS sample divided by the number of galaxies contained in WISE and SDSS. The WISE luminosity function is furthermore also weighted

with the collision weights calculated from the SDSS data and divided by the average fiber collision weight. As we saw from Section 3.2 the high signal-to-noise ratios of our data indicate that we don't need to worry about also weighting by some selection function in WISE; if a galaxy could be matched between WISE and SDSS, it had reliable infrared photometry in WISE. This makes the process of creating an infrared luminosity function almost the same as the optical luminosity function.

5. RESULTS AND DISCUSSION

5.1. SDSS Color-Magnitude Diagrams

We made optical color-magnitude diagrams using data exclusively from the SDSS. These absolute magnitudes include full K-corrections. From Figure 7 we can get a good idea of the spread of color in optical wavelengths for our sample of galaxies, with the difference in color (which was defined as $M_{g^{0.1}} - M_{i^{0.1}}$) spanning about a magnitude. The redness of a galaxy increases along the positive vertical axis, while the luminosity of a galaxy increases towards increasingly negative values along horizontal axis of our plot. There seems to be a bimodality in the color distribution of galaxies, with a group of redder which galaxies displaying a greater difference between $M_{g^{0.1}}$ and $M_{i^{0.1}}$ than the bluer ones. Figure 7 also implies that the most luminous galaxies are redder, and the red galaxies also appear to be a better-defined group.

In contrast, the absolute magnitudes for the optical bands have been plotted in Figure 8 without K-corrections. As a result there is a noticeable distortion in the

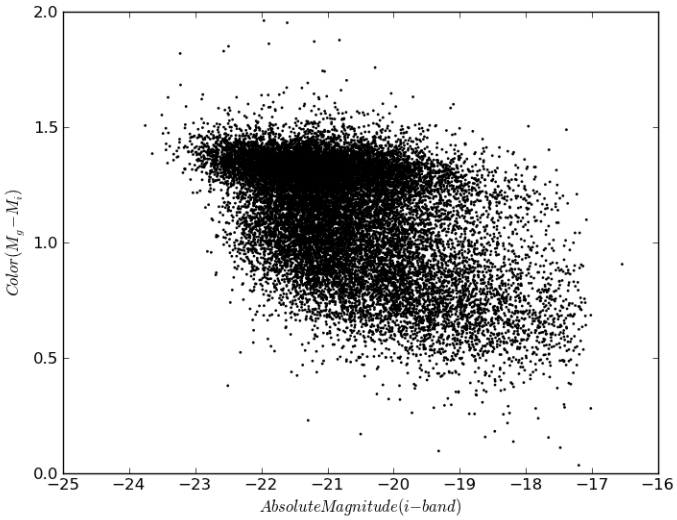

Fig. 7.— The optical color-magnitude diagram using absolute magnitudes from the LSS data samples. This is only 20,000 of the galaxies so that the structure of the plot can be seen. The farther up on the y-axis, the redder the galaxies. As we can see, the most luminous galaxies are also redder and more concentrated.

shape of the color-magnitude diagram due to the lack of K-corrections. This strong dependence on K-corrections also shows us another of the disadvantages of using an optical galaxy survey, since in practice it is difficult to compute an accurate K-correction. However, this diagram still follows the same general trends as Figure 7. As we have seen from Figure 7, the most luminous galaxies are also quite red, and this has been exaggerated without K-corrections.

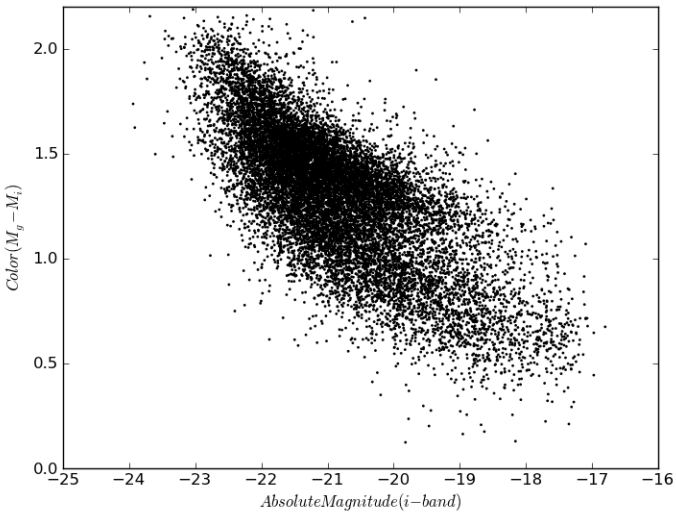

Fig. 8.— The optical color-magnitude diagram using absolute magnitudes that have not been K-corrected. As we can see when comparing this to the previous figure, there is noticeable distortion.

5.2. WISE Color-Magnitude Diagrams

We calculate the luminosities for all of the WISE data by taking the apparent magnitude and subtracting off the distance modulus and approximate K-corrections. These are the luminosities used for the WISE data in all of the plots. The optical luminosities are again taken from SDSS. Figure 9 shows the slightly wider range of luminosities in the 3.4 μm band of WISE than in the $i^{0.1}$-band when plotted against the same optical color range as in Figure 6. But the shape of the color-magnitude diagram is very similar so there seems to be some correlation between optical luminosity and infrared luminosity.

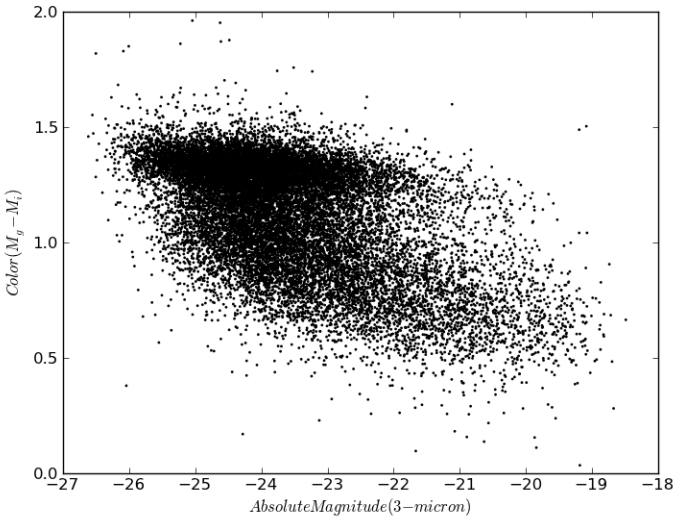

Fig. 9.— The optical color-magnitude diagram (of 20,000 galaxies) using optical magnitudes from the LSS data samples and plotted against the WISE absolute magnitudes. Again, we see that the most luminous galaxies are also redder. Note that the absolute magnitude scale is goes through a similar range of magnitudes in both cases, but this looks more elongated.

Figure 10 shows the infrared color-magnitude diagram plotted against the infrared 3.4μm band. Again, it seems that the most luminous galaxies are also the reddest–we can clearly see a downward slope in the range of redness as the intrinsic luminosities decrease. This slope had also been noticeable in the red part of the optical color-magnitude diagrams. The two groupings of "red" and "blue" galaxies are now gone, but the range of color has remained about the same–this is a little broader, extending about 1.5 magnitudes.

The next plot, Figure 11, shows us the spread in colors in the optical and

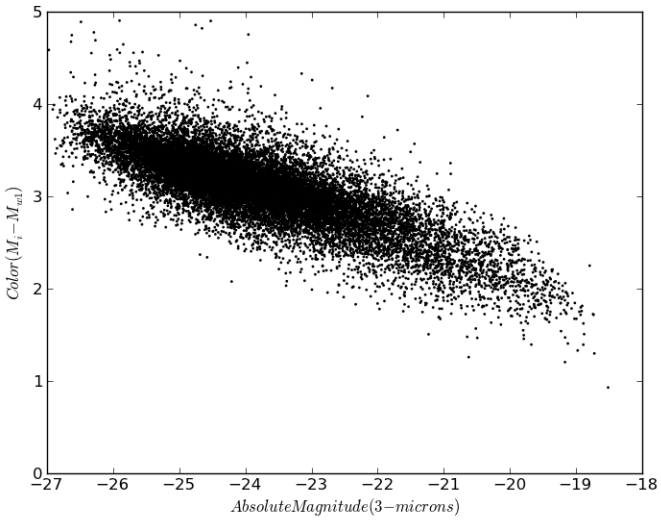

Fig. 10.— $M_{i^{0.1}} - M_{W1}$ plotted against absolute magnitude in the 3-micron band, with redness increasing along the vertical axis. As in the optical color magnitude diagram, we can see that more luminous galaxies are also redder.

infrared regimes. We can see that there is a broader range in the infrared, about 2 magnitudes, compared with roughly 1 magnitude in the optical. We also see that there is a general trend between redness in the infrared and redness in the optical. A similar plot is Figure 12 which reveals about the effect redshift has on color. This color-magnitude was plotted for a narrow range of $i^{0.1}$-band absolute magnitudes, $-21.5 < M_i < -22.5$, and for three different redshift bands. The blue points have $0.05 < z < 0.07$, the black points $0.09 < z < 0.11$, and the red points have $0.17 < z < .20$. We make cuts of the absolute magnitude because the farthest away (galaxies with the highest z) will also be the most luminous, and as we have seen from the earlier color-magnitude diagrams, luminous galaxies tend to be redder

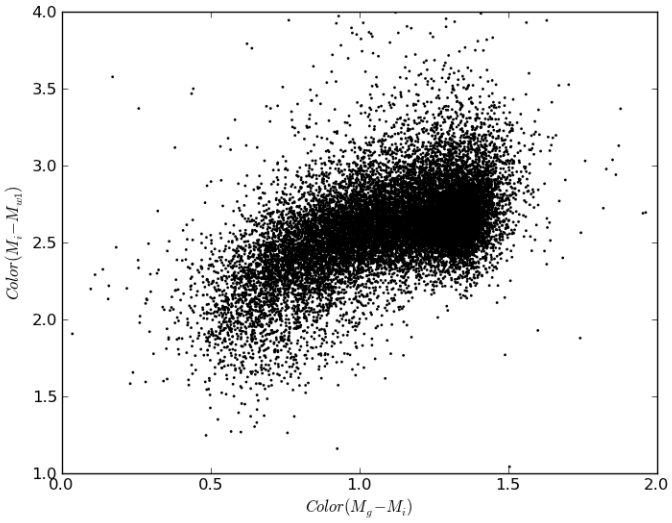

Fig. 11.— A plot of the color $M_{g^{0.1}} - M_{i^{0.1}}$ on the horizontal axis and $M_{i^{0.1}}$-M_{W1} on the vertical axis. This shows that there is a correlation between red in the optical and red in the infrared.

in color. Because these points represent a small range of intrinsic luminosities, we have grouped galaxies that are similar except for their redshifts. However, there is still a difference between galaxies with higher redshift and lower redshift. The three sections seem to not fully align (if they did, they should cover each other up entirely).

The dominant cause of this difference in color over a range of redshifts is likely the result of the small aperture sizes used in WISE. While we are comparing very similar galaxies across different redshifts, these galaxies are also quite intrinsically luminous. The galaxies in the smaller redshift range are closer to us, and as a result also subtend more of the sky than would their higher-redshift counterparts. This

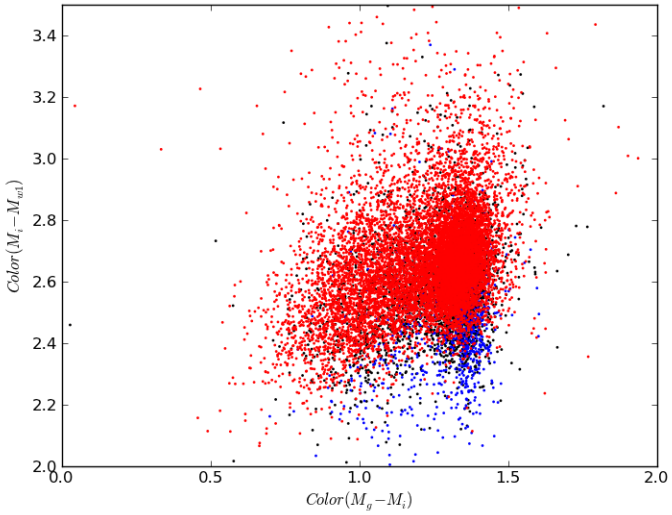

Fig. 12.— A plot of the color $M_{g^{0.1}} - M_{i^{0.1}}$ on the x-axis and $M_{i^{0.1}}$-M_{W1} on the y-axis. The points are color-coded by redshift with blue points being $0.05 < z < 0.07$, black points $0.09 < z < 0.11$, and red $0.17 < z < .20$. This is plotted for a narrow range of i-band absolute magnitudes, $-21.5 < M_{i^{0.1}} < -22.5$. We see that there is still a slight dependence on redshift of color. This is probably due to the difference in aperture sizes used in WISE and SDSS. The WISE magnitudes are calculated using a standard aperture size of 8.25 arcseconds whereas SDSS apertures sizes varied based on the galaxy's light curve. Since the galaxies in our plot are relatively similar (they all had roughly the same luminosity) their points should cover each other, but they do not in our plot. Nearby galaxies may appear bluer because the apertures in WISE may be too small to contain all of the galaxy's flux. Computing more accurate K-corrections may also help with this problem but the dominant reason is most likely the apertures size used in WISE.

means that the smaller aperture likely does not contain all of a galaxy's flux in the W1-band of WISE (we did not have these problems with the SDSS, which used varying aperture sizes for the galaxies) photometry data. Nearby high-luminosity galaxies would then appear to have a lower luminosity in the W1-band than their more distant counterparts. This gives us the apparent relationship between color and redshift despite selecting for galaxies in a narrow band of magnitudes. We should be able to fully correct for this by using the proper aperture sizes for our galaxies and making full K-corrections for the data.

5.3. SDSS r-band Luminosity Function

The SDSS $r^{0.1}$-band luminosity function has already been studied in great detail in previous papers including in Blanton et al. (2001), Blanton et al. (2003), and Bell et al. (2003). We have calculated it again here as a test to see how well our luminosity function corresponds with previous results. This allows us to check that the method we use in making the W1 luminosity function is sound (since a luminosity function has not yet been made for the W1-band we cannot make a direct comparison to the W1-band luminosity function) and also allows us to make more straightforward comparisons between the $r^{0.1}$-band and W1-band luminosity functions.

The $r^{0.1}$-band luminosity function is plotted with number density per h^3 Mpc^3 against the absolute magnitudes, with each bar spanning 0.2 of a magnitude. This was made using only data from the SDSS. The galaxies were each weighted by $1/V_{\rm max}$ and the fiber collision weights as described in Section 4.1. The luminosity

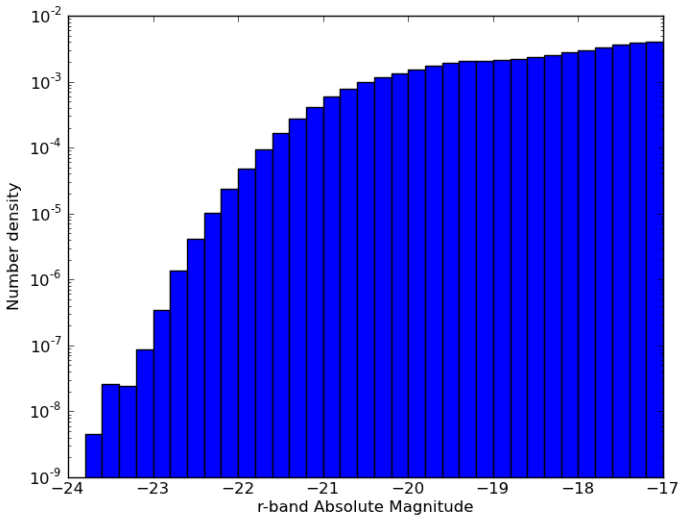

Fig. 13.— The SDSS $r^{0.1}$-band luminosity function. The bars on the histogram span 0.2 of a magnitude. We found that this luminosity function had a luminosity density of about $j \approx 1.75 \times 10^8 h\, L_\odot$ Mpc^{-3}. The comparison between this and the results of the Blanton et al. 2003 and Bell et al. 2003 papers is discussed in Section 5.3 and Figure 15.

function shows a much higher number density of galaxies with higher absolute magnitudes despite the fact that there were fewer less luminous galaxies in our sample itself (this is demonstrated by Figure 3 which shows the number of galaxies in each absolute magnitude range in our sample). We calculate a luminosity density of $j \approx 1.75 \times 10^8 h\, L_\odot$ Mpc^{-3} using

$$L_i = 10^{-0.4(\mathrm{M}_i - \mathrm{M}_\odot)} \tag{7}$$

Where L_i is the luminosity (in solar luminosities) of a single galaxy and $\mathrm{M}_\odot$

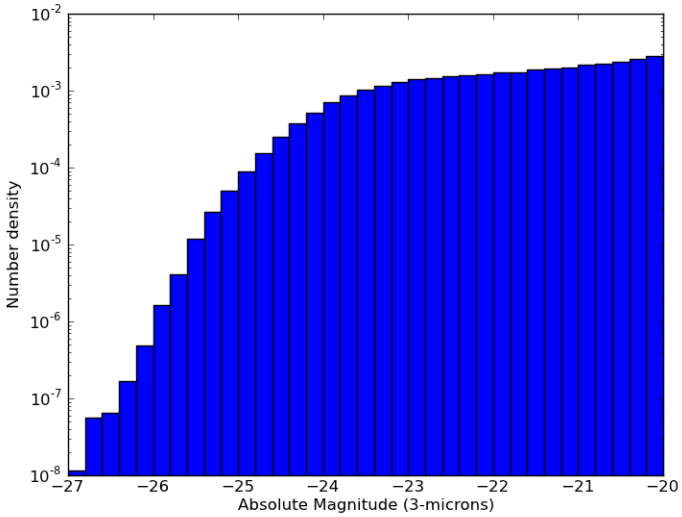

Fig. 14.— The WISE W1 luminosity function. The bars on the histogram span 0.2 mag. We found that this luminosity function had a luminosity density of about $j \approx 6.605 \times 10^8 h\, L_\odot$ Mpc^{-3}. This comparison between this and the results of Bell et al. 2003 and Kochanek et al. 2001 are discussed in Section 5.4 and Figure 15.

is the absolute magnitude of the Sun in the bandpass corresponding to our galaxy measurements. Since our sample has a bandshift of $z = 0.1$ we use the absolute magnitude of the Sun with a bandshift of $z = 0.1$. This is $M_{r0.1\odot} = 4.76$ mag (Blanton et al. 2003). From this we can calculate a luminosity density, j where

$$j = \sum_i \frac{1}{V_{\max}}_i f_i L_i \ . \tag{8}$$

Where f_i is the SDSS selection function. Thus the luminosity density has been weighted by the same weights we applied to our $r^{0.1}$-band luminosity function. This luminosity density is slightly different from previous results. Blanton et al.

	r-band Luminosity Density	W1-band Luminosity Density
Calculated	$1.75 \times 10^8\, h\, L_\odot Mpc^{-3}$	$6.605 \times 10^8\, h\, L_\odot Mpc^{-3}$
Kochanek et al. 2001	-	$7.14 \pm 0.75 \times 10^8\, h\, L_\odot Mpc^{-3}$ (K-band)
Bell et al. 2003	$1.80^{+0.03}_{-0.08} \times 10^8\, h\, L_\odot Mpc^{-3}$	$5.8^{+1.8}_{-0.1} \times 10^8\, h\, L_\odot Mpc^{-3}$ (K-band)
Blanton et al. 2003	$1.84 \pm 0.04 \times 10^8\, h\, L_\odot Mpc^{-3}$	-

Fig. 15.— Luminosity densities for the optical and infrared luminosity functions. We find that the luminosity density in the infrared band is 4 times greater than in the optical. There are slight discrepancies between the values we calculate and the values obtained in the literature. For the optical luminosity function the evolution of the data set–Blanton et al. 2003's paper uses the second SDSS data release while our data comes from the seventh SDSS data release and contains considerably more galaxies–may have contributed to the difference in luminosity densities. Our r-band luminosity density falls into the error bars of the value calculated in Bell et al. 2003. The W1-band (centered at 3.4μm) and K-band (centered at 2.2μm) luminosity densities are not completely analogous, but our result for the W1-band still falls within the error bars of Kochanek et al. 2001 and Bell et al. 2003's results. The previous results were also based on a much smaller sample of galaxies.

(2003) found a luminosity density of $j \approx 1.84 \pm 0.04 \times 10^8 h\, L_\odot$ Mpc^{-3} using the same value for M$_\odot$, while Bell et al. 2003 found a luminosity density value of $j \approx 1.80^{+0.03}_{-0.08} \times 10^8\, h\, L_\odot Mpc^{-3}$. Our value for luminosity density falls into Bell et al.'s error bars but not within Blanton et al.'s. It is possible that since our sample contains over 500,000 galaxies, and Blanton's contained about 150,000 galaxies that the parameters of the sample have simply changed over time with the inclusion of more points. Figure 15 summarizes these results.

5.4. WISE 3-micron Luminosity Function

Figure 14 shows the WISE W1-band luminosity function. As described in Section 4.1, this has been weighted by $1/V_{\rm max}$, the fiber collision weights, and the ratios of the number of galaxies in the original sample and in WISE. It bears a fairly strong resemblance to the luminosity function in the optical. The WISE luminosity function is only complete to absolute magnitudes of about -20 because of the absolute magnitude cuts placed on the galaxies originally from the SDSS. The $r^{0.1}$-band absolute magnitude of our galaxies were cut off at a minimum absolute magnitude of -17, which did not translate into a sharp cutoff of absolute magnitudes in the infrared band and thus caused an artificial "turn-down" in the lower luminosities of our WISE luminosity function. Since we do not know exactly to what extent this has affected our infrared luminosity function, we have estimated that our luminosity function is only complete to about -20 mag. From this luminosity diagram, we calculate $j \approx 6.605 \times 10^8 h\, L_\odot$ Mpc^{-3}, using $M_\odot \approx 3.25$ mag. This value was approximated using the absolute magnitude of the Sun in the

K-band, $M_K = 3.33$, which was taken from Allen's Astrophysical Quantities. This value for $M_\odot$ has an error of about ± 0.05 mag.

Kochanek et al. (2001) calculated a K-band luminosity density of $j \approx 7.14 \pm 0.74 \times 10^8 h\, L_\odot$ Mpc^{-3} and Bell et al. 2003 calculated a K-band luminosity density of $j \approx 5.8^{+1.8}_{-0.1} \times 10^8 h\, L_\odot$ Mpc^{-3}. Since the K-band is centered on 2.2μm it is not quite the same as the W1-band, which is centered on 3.4μm. However our W1-band luminosity density still falls within the error bounds of both of the previously calculated K-band luminosity density values, so the luminosity density value we got for the W1-band seems reasonable. Since the value for $M_\odot$ in the W1-band was only an approximation, we may have error from this value that could have caused our answer to be different from the previous results.

6. CONCLUSIONS

We found that the infrared luminosity density is higher than the optical luminosity density by a factor of 4. The greater luminosity density in the infrared is due in part to the difference in color between the Sun and an average galaxy. The Sun is more luminous in shorter wavelengths so it has a lower absolute magnitude in bluer wavelengths. Since the Sun is less luminous in longer wavelengths, galaxies in longer wavelengths also have a greater solar luminosity density. If our Sun were redder than the average galaxy, then we would see the opposite trend occur; redder galaxies would have smaller luminosity densities than bluer galaxies. The other cause of a greater luminosity density at longer wavelengths is the addition of light from giant, post-main sequence stars, which are very luminous in the infrared

wavelengths, but not in the optical wavelengths. These factors both help explain the increase in infrared luminosity density over optical luminosity density.

Studying and understanding the infrared luminosity function will be crucial to developing our understanding of the formation and evolution of galaxies. We have used one of the most comprehensive infrared galaxy surveys, WISE, to create a luminosity function containing many more galaxies than previously possible. Previous studies into the infrared luminosity function were hampered by the lack of infrared sky surveys with breadth of WISE. The infrared luminosity function will allow us to get better estimates of stellar mass, since it is less sensitive to extinction and to recent star formation.

Since I began working on this project, more data has been released from WISE. The first WISE data release overlapped with only a fraction of the original SDSS sample data; a natural next step would be to make the luminosity function using the WISE infrared data for all of the galaxies in the sample. We have also not yet made the full K-corrections for the WISE data, only approximations. Though they are less important in the infrared than in the optical, they still produce noticeable effects in our results. To get more accurate results, it would be necessary to compute the K-corrections more carefully in the future.

Finally, the manner in which the magnitude measurements are recorded in the WISE data make it more difficult to get accurate magnitude measurements of the bigger and brighter galaxies, because we are using the magnitude measurements from a fixed aperture radius ($8.25''$) in our measurements. We have already seen the effect that this has had on the color of galaxies with lower redshift. We can try to

improve this in the future by finding the apertures were used for the galaxies in the SDSS data and then picking the magnitude measurement in the WISE data from an aperture of similar size. This should give us apertures that will contain more of a galaxy's flux that we are currently able to get and improve the accuracy of our calculations.

7. ACKNOWLEDGEMENTS

This was far from a completely independent research project, so I would like to thank all those that helped me with the paper, the presentation, and the research. I would like to thank my advisor Professor Daniel Eisenstein for his patience and guidance, without which this project would not have been possible, Professor Edo Berger for his advising and direction in Astronomy 98, which helped me prepare for presenting my work, Professor Robert Kirshner for being my external reader and giving me very good suggestions on how to improve my paper, my friend Diana Cai who helped me get started with learning Python, and my classmates in Astronomy 98 who have listened to me talk about my project over the course of the semester.

This publication makes use of data products from the Wide-field Infrared Survey Explorer, which is a joint project of the University of California, Los Angeles, and the Jet Propulsion Laboratory/California Institute of Technology, funded by the National Aeronautics and Space Administration.

REFERENCES

Assef, R. J., et al., AJ, 676, 286 (2008)

Assef, R. J., et al., AJ 713, 970 (2010)

Bell, E. F., and de Jong, R.S., AJ, 550, 212 (2001)

Bell, E. R., et al., AJ, 149, 289 (2003)

Blanton, M. R., et al., AJ, 121, 2358 (2001)

Blanton, M. R., et al., AJ, 592, 819 (2003)

Blanton, M. R., et al., AJ, 129, 2562 (2005)

Conroy, C., Gunn, E., & White, M., AJ, 699, 486 (2009)

Kochanek, C.S., et al., AJ, 560, 566 (2001)

Hogg, D. W., et al. (2002)

Moustakas, J., et al., AJ (2011)

Wright, E. L., et al., AJ, 140, 1868 (2010)

York, D.G., et al., AJ, 120, 1579 (2000)

This manuscript was prepared with the AAS LaTeX macros v5.2.